localization in the newly regenerated nuclei at telophase depends on Lam. Arrowheads in D and E indicate duplicated centrosomes characteristic of late telophase I cells. Bar; 10μm.

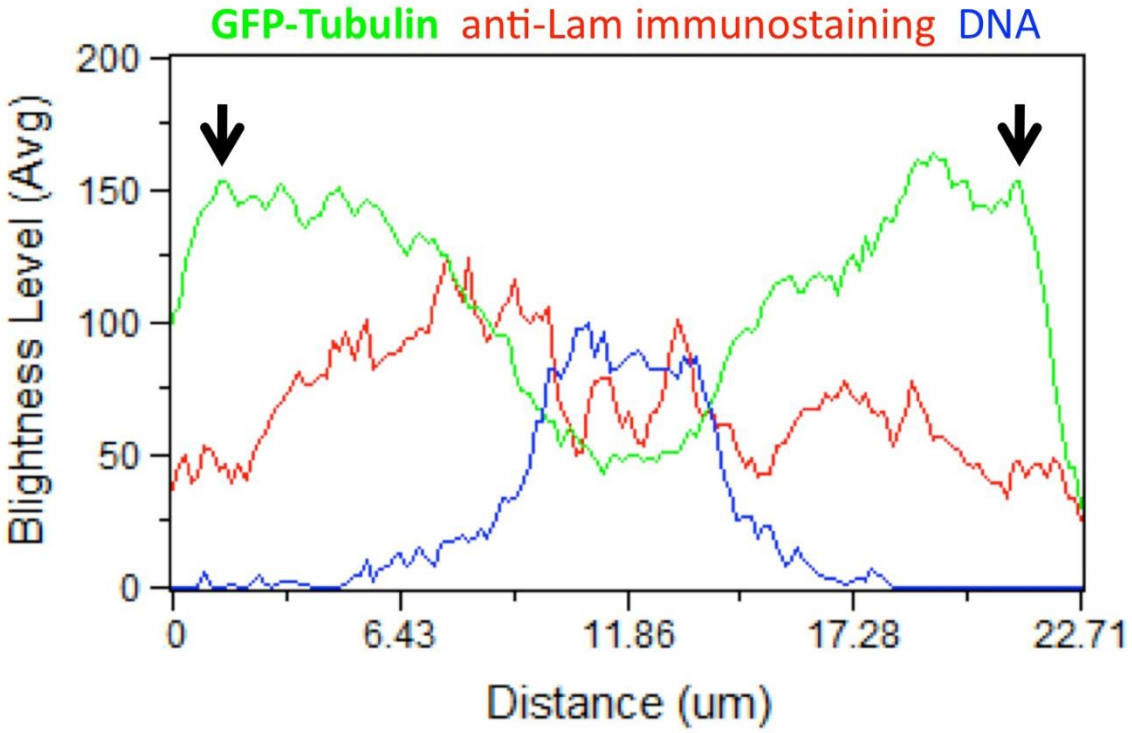

Fig. S4. A distribution of Lam (red), microtubules (green) and DNA (blue) within the metaphase I spermatocyte appeared in Fig. 1D. Fluorescence intensity of anti-Lam immunostaining signal, GFP-Tubulin fluorescence and DAPI fluorescence on the horizontal line drawn between two spindle poles (arrows) was measured by linescan software. Note that the Lam signal decreased in amount around spindle poles, suggesting that the metaphase cell was devoid of Lam nuclear lamina around spindle poles.

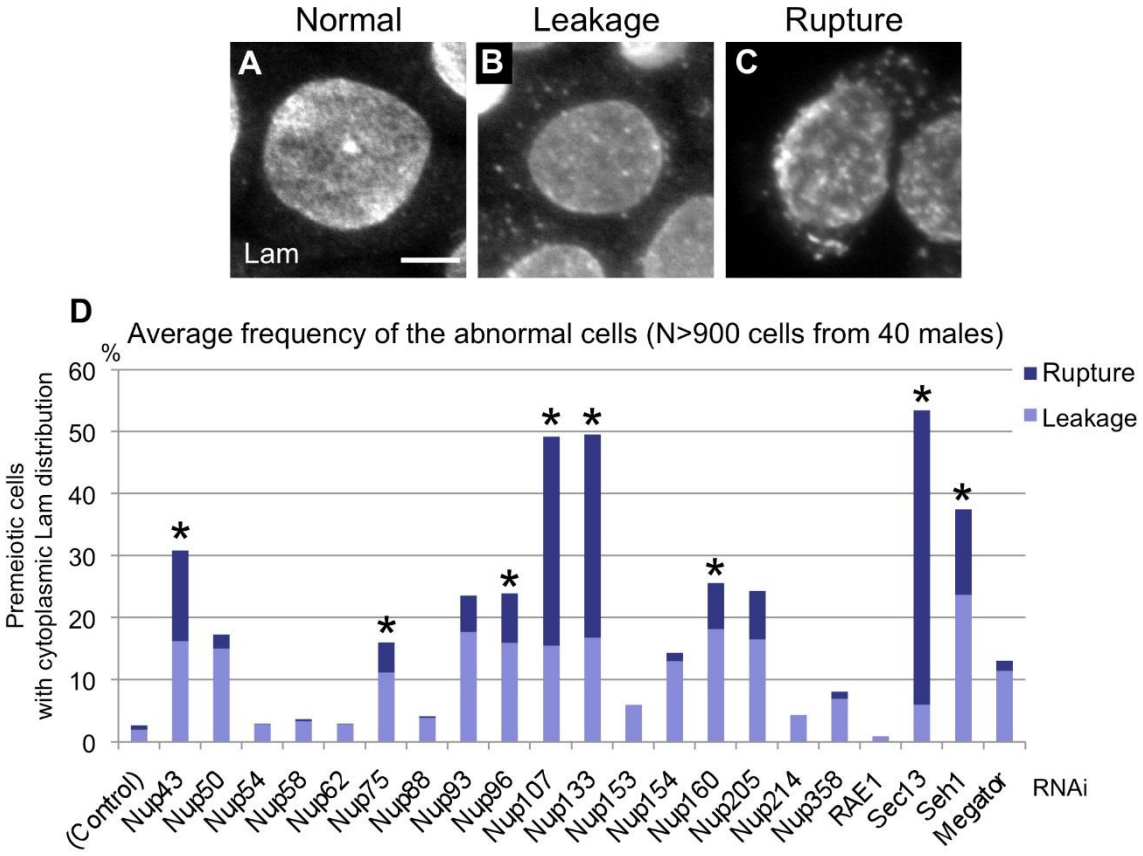

Fig. S5. Expression of dsRNA for several individual components of the NPC results in precocious disintegration of Lam lamina before meiotic initiation. (A-C) Anti-Lam immunostaining of the nuclear lamina consisting of the B-type lamin in premeiotic cells from mature spermatocyte cysts. (A) A normal control spermatocyte with dsRNA expression against GFP. (B, C) Nup107-depleted cells showing two types of nuclear phenotype. (B) A less severe "leakage" phenotype in which many small foci labeled by anti-Lam immunostaining was observed throughout the cytoplasm. (C) A more severe "rupture" phenotype in which pieces of nuclear lamina became detached from the nucleus. Bar; 10 μ m. (D) Summary of nuclear phenotypes of spermatocytes expressing testis-specific dsRNA for each of 21 NPC components (N>900 premeiotic spermatocytes at S5 stage from 40 males for each). Expression of a representative component for each NPC subunit (Nup62, Nup93, Nup107, Nup153 and Nup358) was examined by the qRT-PCR and confirmed that the dsRNA expression reduced the amount of their mRNAs. Average frequencies of abnormal premeiotic spermatocytes

showing the rupture phenotype and those showing the leakage phenotype were presented on the y-axis. Note that depletion of Nup107 and dsRNA expression of seven other members of the Nup107-160 complex (marked with asterisks) resulted in the appearance of the abnormal nuclear phenotypes at a higher frequency.

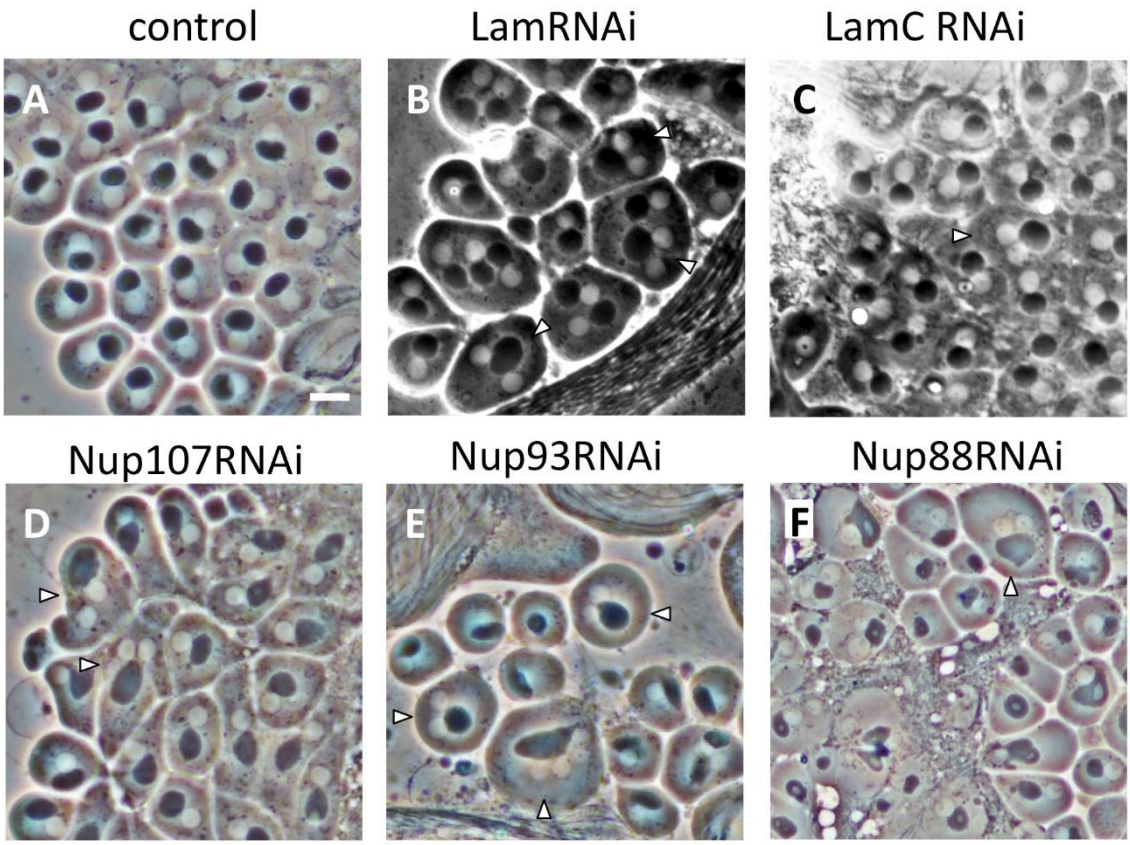

Fig. S6. Representative images of spermatids depleted of each gene encoding Lamins and Nups after completion of meiosis II. (A) Control spermatids at the onion stage. (B) Onion stage spermatids from a Lam-depleted testis. (C) Onion stage spermatids from a LamC-depleted testis. (D) Onion stage spermatids from a Nup107-depleted testis. (E) Spermatids from a Nup93-depleted postmeiotic cyst just after the onion stage. (F) Onion stage spermatids from a Nup88-depleted testis. Arrowheads indicate multinucleate cells containing single larger Nebenkerns, which are the consequences of a failure of cytokinesis during a meiotic division(s). Bar: 10 μm.

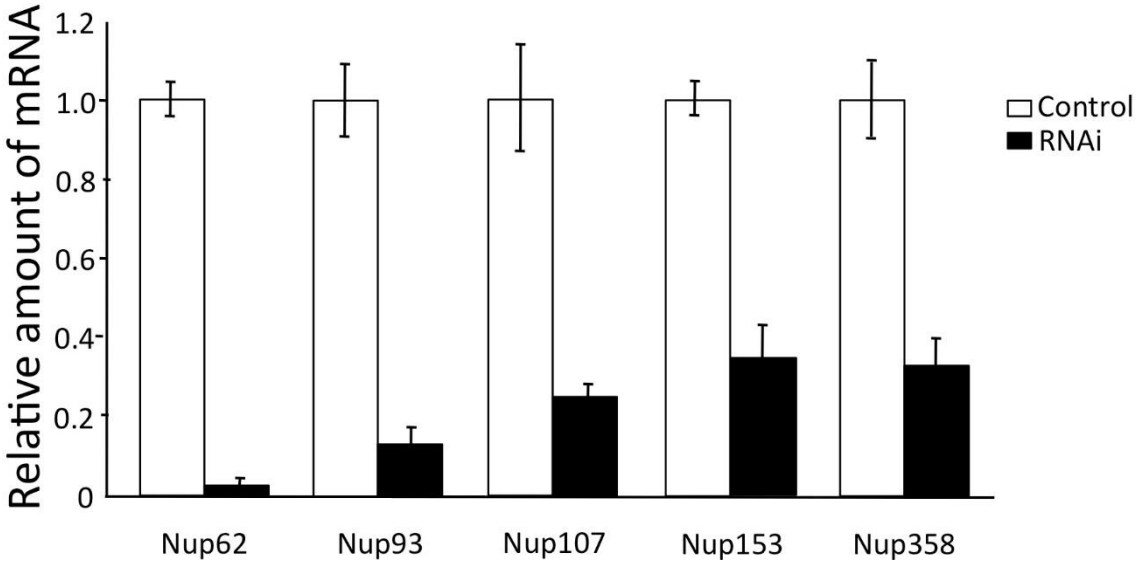

Fig. S7. The dsRNA expression for Nup62, Nup93, Nup107, Nup153 and Nup358 resulted in efficient depletion of each mRNA. Depletion efficiencies of each dsRNA were estimated by a real time qRT- PCR. The mRNA level of the adult testes from control flies (bam-Gal4>GFP RNAi), and flies with each dsRNA expression (bam-Gal4>Nup62 RNAi, bam-Gal4>Nup93 RNAi, bam-Gal4>Nup107 RNAi, bam-Gal4>Nup153 RNAi, bam-Gal4>Nup358 RNAi), as normalized to the control. Data are represented as averages of three independent experiments and error bars represent the standard deviation.

Table S1. Quantification of meiotic defects appeared in onion stage spermatids from spermatocytes with dsRNA expression of each gene for Lamins and the Nups.

dsRNA expression	Nebenkern-to-nuclei ratio						Frequency of meiotic defects (%)	
	Normal(%)	Abnormal (%)					Multinucleate *1	Various nuclear size*2
	1:1	1:0	1:2	1:3	1:4	1:>5		
GFP(Control)	96.30	0.78	2.73	0.10	0.10	0.00	2.93	0.49
Lam	73.53	1.29	17.56	3.22	3.77	0.64	25.18	3.77
LamC	94.88	1.54	3.18	0.41	0.00	0.00	3.59	1.43
Nup43	77.32	3.93	15.71	2.50	0.36	0.18	18.75	5.00
Nup50	74.06	2.18	18.61	3.56	1.39	0.20	23.76	9.50
Nup54	Cell cycle arrest*3							
Nup58	Cell cycle arrest*3							
Nup62	Cell cycle arrest*3							
Nup75	83.98	1.05	13.07	0.63	1.16	0.11	14.9 6	0.95
Nup88	75.53	1.86	18.26	2.98	1.12	0.25	22.61	7.08
Nup93	62.40	7.44	26.45	3.31	0.00	0.41	30.17	10.74
Nup96	61.22	5.90	26.98	4.08	1.36	0.45	32.88	7.94
Nup107	85.67	3.89	8.78	1.44	0.14	0.07	10.44	5.33
Nup133	81.38	1.07	15.91	1.26	0.39	0.00	17.56	1.75
Nup153	80.64	4.48	10.25	3.20	1.07	0.36	14.88	7.62
Nup154	Cell cycle arrest*3							
Nup160	72.73	4.43	19.29	2.00	1.55	0.00	22.84	4.21
Nup205	82.03	3.42	13.92	0.63	0.00	0.00	14.56	3.16
Nup214	74.16	4.42	16.46	3.72	1.06	0.18	21.42	11.50
Nup358	74.08	5.48	10.77	5.08	2.19	2.39	20.44	12.36

Rae1	Cell cycle arrest*3							
Sec13	55.80	4.27	29.69	3.92	3.58	2.73	39.93	5.46
Seh1	78.31	1.39	15.89	2.65	1.51	0.25	20.30	5.17
Megator	96.56	0.49	2.95	0.00	0.00	0.00	2.95	0.20

More than 500 onion-stage spermatids in testes from 20 males were examined about the Nebenkern-to-nuclei ratio per each genotype. *1 All the spermatids carrying abnormally large Nebenkern associated with more than 2 nuclei were summarized. They are considered to be derived from a failure of cytokinesis in both or each of two meiotic divisions. *2All the spermatids containing larger or smaller nuclei were separately counted and summarized in this category. They would be a consequence of unequal chromosome segregation in meiotic divisions. *3Any meiotic cysts failed to be observed in the testes with dsRNA expression of Nup54, Nup58, Nup154 or Rae1.

Table S2. A list of the UAS stocks used in this study.

Name	ID number	Collection	References
UAS-Lam RNAi	107419	VDRC	
UAS-LamC RNAi	31621	Bloomington	
UAS-Nup43 RNAi	108595	VDRC	Muerdter, et al., 2013
UAS-Nup50 RNAi	100564	VDRC	
UAS-Nup54 RNAi	103724	VDRC	Czech et al., 2013
UAS-Nup58 RNAi	108016	VDRC	
UAS-Nup62 RNAi	100588	VDRC	
UAS-Nup75 RNAi	27495	VDRC	Mummery-Widmer, et al., 2009
UAS-Nup88 RNAi	47691	VDRC	Neumüller et al., 2011
UAS-Nup93 RNAi	100315	VDRC	Mummery-Widmer, et al., 2009
UAS-Nup96 RNAi	109279	VDRC	
UAS-Nup107 RNAi	110759	VDRC	
UAS-Nup133 RNAi	110194	VDRC	
UAS-Nup153 RNAi	107750	VDRC	
UAS-Nup154 RNAi	106136	VDRC	Muerdter, et al., 2013
UAS-Nup160 RNAi	109318	VDRC	
UAS-Nup205 RNAi	38608	VDRC	
UAS-Nup214 RNAi	41964	VDRC	
UAS-Nup358 RNAi	38581	VDRC	Mummery-Widmer, et al., 2009
UAS-Seh1 RNAi	106489	VDRC	
UAS-GFP RNAi	9330	Bloomington	
UAS-RAE1 RNAi	9862R-2	NIG-fly	Montgomery et al., 2014
UAS-Sec13 RNAi	6773R-1	NIG-fly	
UAS-Megator RNAi	8274R-2	NIG-fly	